

# Reliability of IGBT in a STATCOM for Harmonic Compensation and Power Factor Correction

Lakshmi Gopi Reddy, Leon M. Tolbert

Department of Electrical Engineering and Comp. Sci.  
University of Tennessee,  
Knoxville, USA.  
Email: lgopired@utk.edu

Burak Ozpineci, Yan Xu, D. Tom Rizy

Oak Ridge National Laboratory  
Oak Ridge, USA.

**Abstract**—With smart grid integration, there is a need to characterize reliability of a power system by including reliability of power semiconductors in grid related applications. In this paper, the reliability of IGBTs in a STATCOM application is presented for two different applications, power factor correction and harmonic elimination. The STATCOM model is developed in EMTP, and analytical equations for average conduction losses in an IGBT and a diode are derived and compared with experimental data. A commonly used reliability model is used to predict reliability of IGBT.

## I. INTRODUCTION

With the integration of Smart Grid (SG) technology into the bulk power system, the issue of reliability of the system is a matter of concern. North American Electric Reliability Corporation (NERC), the Electric Reliability Organization (ERO) certified by Federal Energy Regulatory Commission (FERC) to establish and enforce reliability standards for the bulk power systems, in its report on “Reliability Considerations from Integration of Smart Grid,” has emphasized all the existing devices and systems such as Phasor Measuring Units, Flexible AC Transmission Systems (FACTS), etc., for assessing reliability of the bulk power system [1]. According to an industry based survey presented in [2], the power semiconductor device failures are a major concern for reliability of the power converter. According to MIL-std, the IGBTs are the second most unreliable devices causing failure of the inverter, after capacitors [14].

There is a need to study the individual reliability of these devices/systems to predict their impact on the grid. This research mainly focuses on the reliability of power semiconductor devices, Insulated Gate Bipolar Transistor (IGBT) devices, in particular, used in the power electronics devices integrated with power systems.

Reliability of power semiconductors in power converters in traction application is a widely researched topic especially

in Europe, initiated by as a part of the RASPDRA and LESIT, projects. Recent IGBT reliability applications included inverters integration for PV and wind applications, adjustable speed drives, matrix converters, electric vehicle applications, aerospace applications etc. [2-8]. Little research has been found in reliability of IGBTs and the power converters in FACTS applications.

A system overview for estimating the lifetime of IGBTs is presented in Fig. 1. For the electrothermal model, the data from device characteristics and the operating condition values are input from the characteristic tests and from the simulation model. The power losses are calculated and the thermal model of the IGBT is used to estimate junction temperatures. From temperature profiles, the lifetime prediction model is developed. Finally, the lifetime estimation is complete after verification from accelerated lifetime testing experiments.

A simple two-bus system was developed with source and load as shown in Fig. 2. A three-phase sinusoidal voltage source,  $V_s$ , of 480 V line-line voltage is connected to a load drawing a current,  $i_l$ . The STATCOM is connected in shunt between the source and load via a coupling inductance  $L_c$ , so that it provides the necessary reactive current for the respective functions of the STATCOM such as power factor correction, harmonic elimination, etc. The controller of the STATCOM in this work is based on non-active power compensation theory [8]. The model of the system is developed in EMTP software.

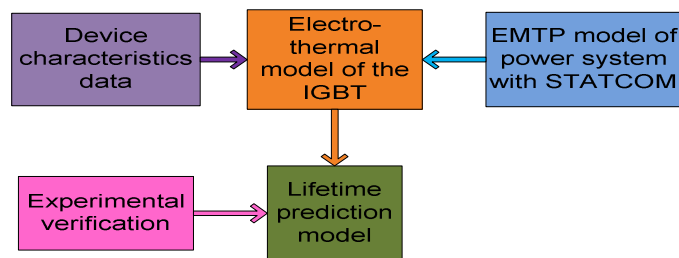


Figure 1. System overview and methodology of estimating lifetime of IGBTs.

Prepared by the Oak Ridge National Laboratory, Oak Ridge, Tennessee 37831, managed by UT- Battelle for the U.S. Department of Energy under contract DE-AC05-00OR22725.

The submitted manuscript has been authored by a contractor of the U.S. Government under contract DE-AC05-00OR22725. Accordingly, the US Government retains a non-exclusive, royalty-free license to publish from the contribution, or allow others to do so, for U.S. Government purposes.

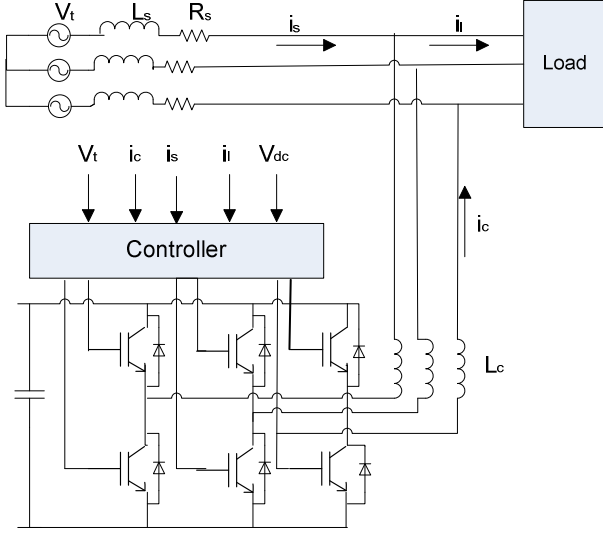


Figure 2. Two bus model of power system with shunt connected STATCOM.

## II. LOSS CALCULATION

### A. Analytical Calculation

Table I describes the list of parameters used for analytical calculation methodology.

#### 1) Power Factor Correction

When an inverter is operating to compensate for reactive power to maintain unity power factor of the grid, the losses are given by [13]

$$(P_{cond_i}) = I_l \times \sin(\phi) \times \left( \frac{V_{on_i}}{2\pi} + \frac{I_l \times R_{on_i}}{8} \right) \quad (3)$$

$$(P_{cond_d}) = I_l \times \sin(\phi) \times \left( \frac{V_{on_d}}{2\pi} + \frac{I_l \times R_{on_d}}{8} \right) \quad (4)$$

#### 2) Harmonic Compensation of Odd Non-Triplen Harmonics

The active current provided by the source is

$$i_{active} = i_s = i_l \cos(\Phi) \cos(\omega t) \quad (5)$$

while the current provided by the inverter by non-active power compensation is

$$i_{nonactive} = i_c = i_l \sin(\Phi) \sin(\omega t) + i_5 \cos(5\omega t) + i_7 \cos(7\omega t) + \dots \quad (6)$$

Control voltage to the PWM is given by [13]

$$V_c = V_s + L_c \frac{di_c}{dt} \quad (7)$$

$$d_{sw} = 0.5 \times \left( 1 + M_1 \times \cos(\theta) - \sum_{h=5,7,11,\dots} M_{2h} \times \sin(h\theta) \right) \quad (8)$$

$$d_d = 0.5 \times \left( 1 - M_1 \times \cos(\theta) + \sum_{h=5,7,11,\dots} M_{2h} \times \sin(h\theta) \right) \quad (9)$$

TABLE I: LIST OF PARAMETERS AND DESCRIPTIONS

$I_l$	load current of the system
$I_a$	inverter phase current
$\Phi$	power factor angle of the load
$M$	modulation index
$R_{fd}$	on state resistance of diode
$R_{oni}$	on state resistance of IGBT
$V_{on_d}$	forward voltage drop across the diode
$V_{on_i}$	forward voltage drop across the IGBT
$E_{on\_test}$	turn on switching losses from test conditions
$E_{off\_test}$	turn off switching losses from test conditions
$V_{DC}$	DC voltage across the switch during the current operation
$V_{DC\_test}$	DC voltage across the switch with the test conditions from the datasheet
$h$	harmonic number
$I_{ctest}$	current across the IGBT during test conditions
$I_h$	$h^{\text{th}}$ harmonic current
$f_{sw}$	switching frequency
PF	power factor of the inverter

$$\text{where } M_1 = \frac{V_s + \omega \times L_c \times I_l \times \sin(\phi)}{\tilde{V}_{tri}} ; M_{2h} = \frac{h \times \omega \times L_c \times I_h}{\tilde{V}_{tri}}$$

$$(i_{sw})_{avg} = \int_0^x i_c \times d_{sw} \times d\theta \quad (10)$$

$$(i_d)_{avg} = \int_0^x i_c \times d_d \times d\theta \quad (11)$$

where  $x$  is the angle at which the current becomes negative and hence the other IGBT conducts.

Similarly, the rms currents,

$$(i_c)_{rms}^2 = (I_l \sin(\Phi))_{rms}^2 + (I_5)_{rms}^2 + I_7^2 + I_{11}^2 + \dots \quad (12)$$

$$(i_{sw})_{rms} = \int_0^x (i_c)_{rms}^2 \times d_{sw} \times d\theta \quad (13)$$

$$(i_d)_{rms} = \int_0^x (i_c)_{rms}^2 \times d_d \times d\theta \quad (14)$$

### B. Thermal Model

Foster model of the IGBT was used for the thermal model as shown in the Fig. 3. The calculation of junction and case temperatures were based on the datasheet values of the thermal resistances of the IGBTs and diodes. The heat sink used by PP150T120 inverter was modeled to characterize temperature nearest to its actual value. The air flow speed is 1500 LFM (Linear Feet per Minute) as stated in the datasheet. The temperature gradient in the device is caused due to the

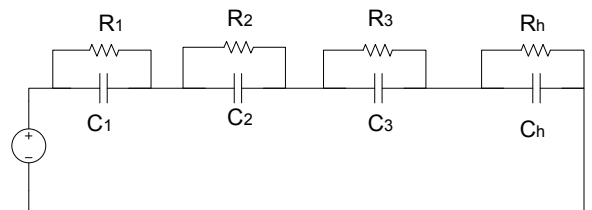


Figure 3. Foster based thermal model of the device.

wave shape of the current and also due to the thermal time constant associated with the thermal model during heating and cooling. It is directly dependent on the power losses in the device. The mean temperature can be obtained by considering the thermal model with purely resistive elements. It is also dependent on the power loss in the device.

### III. SIMULATION RESULTS

#### A. PowerFactor Correction

The IGBT temperature is linearly dependent on the inverter current for reactive compensation. From the analytical equations, this can be attributed more to the high switching losses than conduction losses. Even though the temperature is related to square of the current in the conduction losses, the greater magnitude of switching losses contribute to a more linear relation between current and temperature.

Figure 4 illustrates the junction temperature variation of the IGBT with power factor obtained from linear relation between inverter current and load current and sine of the power factor angle. The negative values of power factor are used to indicate lagging power factor. As the load current increases, the temperature of IGBT also increases [13].

#### B. Harmonic Compensation

##### 1) Single Harmonic Compensation Case:

The losses due to harmonic compensation for a purely harmonic load are independent of the frequency of the harmonics and dependent on the amplitude of the harmonic. From analytical calculations, the average temperature of an IGBT for a purely harmonic load of 40 A of 5<sup>th</sup> harmonics and that for a 40 A of 7<sup>th</sup> harmonics is similar and was verified by simulations. However, there is a decrease in temperature swing  $\Delta T$ , as the frequency increases. This can be explained by the fact that time available for temperature to rise and fall is decreases as the frequency increases. Table II lists the temperature swings and average temperature for odd-non-triplen harmonics of same amplitude simulated as load for the power system shown in Fig. 2.

Fig. 5 shows the temperature waveforms for 5<sup>th</sup> and 7<sup>th</sup> harmonic current compensation of 40A. Their average

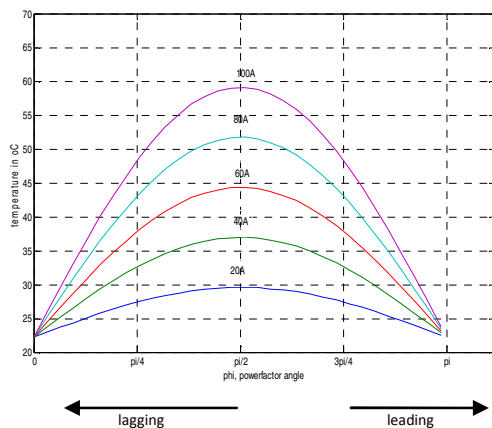


Figure 4. Temperature of IGBT varying with power factor of load.

TABLE II. TEMPERATURE SWING FOR SINGLE HARMONIC CURRENT COMPENSATION OF SAME AMPLITUDE 40 A.

Harmonic #	Tmax	Tmin	$\Delta T$	T <sub>avg</sub>
5	34.2	27.7	6.5	29.7
7	33.0	27.8	5.7	29.7
11	32.2	27.9	4.3	29.7
13	31.9	27.8	4.1	29.7
17	31.5	27.6	3.9	29.7
19	31.2	27.6	3.6	29.7

temperatures are same, even though the temperature swing is smaller for 7<sup>th</sup> harmonic current compensation than that of 5<sup>th</sup> harmonic current compensation.

##### 2) Harmonic Compensation with Phase Difference

For odd non-triplen harmonic compensation with a phase difference, the temperatures of the IGBT and diodes are not significantly different than the temperatures with single harmonic compensation case. This is because, the phase difference for a current at 300Hz, for 5<sup>th</sup> harmonic, is only for a very short duration of time, 0.5ms for 60 degrees phase lag and the small change in temperature due to conduction can be neglected.

##### 3) Diode Bridge Rectifier Case

The diode bridge rectifier based resistive load on the power system was simulated to study the impact of various harmonic current compensation on the temperature of the inverter. Fig. 6 shows the contribution of different combinations of harmonic current compensation towards simulated temperature data. The average current is dependent on the duty cycle of the switch (indirectly dependent on the derivative of the current) and also the time period for which the current is positive [13].

##### 4) Fundamental Reactive Compensation with Harmonic Compensation

A case with a load current constituted by a large lagging fundamental current and a diode bridge rectifier based

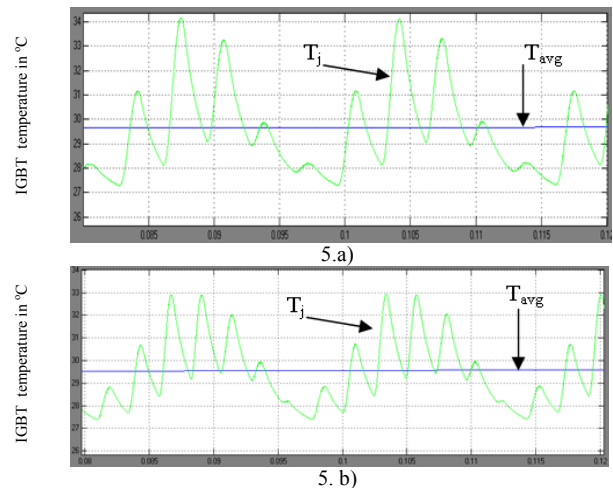


Figure 5. Temperature of IGBT for purely 5.a) 5th harmonic current and 5.b) 7th harmonic current

harmonics of lower magnitudes compared with fundamental was simulated to compare with the temperature with fundamental non-active current compensation. However, due to the predominant effect of the fundamental current, the mean temperature was constant.

In the presence of fundamental current compensation by a STATCOM, the effect of harmonics though is significant on the shape of the temperature waveform, whereas the average temperature and temperature swing are predominantly dependent on the fundamental current component.

#### IV. EXPERIMENTAL SETUP

A STATCOM connected to the 480 V line-line grid is set up, as shown in Fig. 7 at Oak Ridge National Laboratory (ORNL). The inverter, APS PP150T120 consisting of three Powerex IGBT modules (CM150DU-24F) rated at 1200 V, 150 A, is connected to DC voltage source of 800 V. A fan is installed to run at a maximum speed of 1500 LFM for heat removal from the inverter system.

The inverter was tested off-grid to feed purely inductive loads to study its operation for reactive power compensation. A thermistor is placed in the inverter between Phase A and B IGBT modules to monitor temperature. The inverter is controlled using dSPACE and the temperature is monitored.

Fig. 8 compares the temperature data at different inverter loads for reactive compensation by analytical calculation, simulation and experimental results. The analytical data and simulated data are closer than experimental data. The experimental data was from a thermistor placed in between phase A and B and not directly from IGBT module A. The temperature is lower than actual IGBT temperature.

#### V. RELIABILITY MODEL

One of the most common methods of testing reliability of semiconductors is by power cycling tests. The typical model of predicting the number of cycles to failure of an IGBT based power cycling capability is given by Arrhenius and Coffin-Mason laws of degradation [11].

$$N_f(T_m, \Delta T_j) = A \times \Delta T_j^\alpha \times \exp\left(\frac{Q}{RT_m}\right) \quad (15)$$

where  $A$ ,  $\alpha$  are constants and are module dependent,  $R$  is the gas constant (8.314 J/mol.K),  $T_m$  is the mean junction

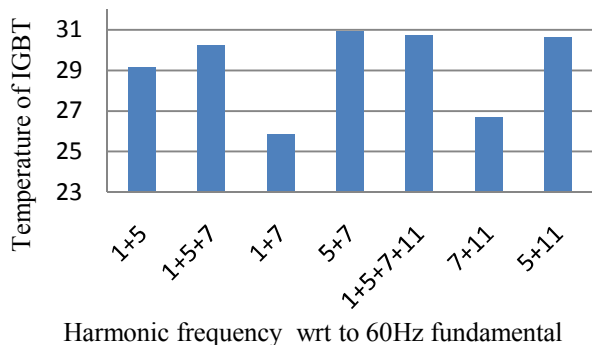


Figure 6. Temperature of IGBT at different harmonic frequency compensation of diode bridge rectifier load of the system.

temperature in one power cycle is in Kelvin, the internal energy  $Q = 7.8 \times 10^4 \text{ Jmol}^{-1}$  (or about 0.8eV).  $\Delta T_j$  is the variation of the junction temperature. By curve fitting the supplier's power cycling data to that of (15), the constants are derived as  $\alpha$  equals -6.14, for mean temperature,  $T_m$  of 25 °C,  $A=1300$ . The constant values were obtained by curve fitting the manufacturer's data for power cycling to (15).

The lifetime of the IGBT from (15) is shown in Fig. 9 for power factor compensation operation by the STATCOM. As the load power factor varies from 1 to 0, the temperature gradient and mean temperature both increase as the power losses increase with inverter current. Hence the lifetime of the IGBT is inverted with respect to the mean temperature profile obtained in Fig. 4

The calculation of lifetime of IGBT for the case when the inverter is compensating for a single harmonic current is shown in Fig. 10 for varying harmonic current. For high frequency harmonics, the temperature gradient is lower and hence the lifetime is higher compared with lower frequency harmonics. For single harmonic compensation by the STATCOM, the mean temperature is independent of the frequency of the harmonic and dependent on the amplitude of the harmonic current.

#### VI. POWER CYCLING

An H-bridge inverter fulfills criteria for power cycling test circuit. However, for high power factor loads, most of the power is dissipated in load and hence the equipment and energy costs for these tests would be very high. A purely reactive load would reduce the costs significantly as the power would be circulating to charge and discharge the load [12]. This is a best suited testing circuit for STATCOM operation, since it mimics the reactive power compensation operation of the inverter. It should be noted that for purely reactive load, the losses in the IGBT are reduced while that of diode are increased compared to the high power factor operation of the inverter.

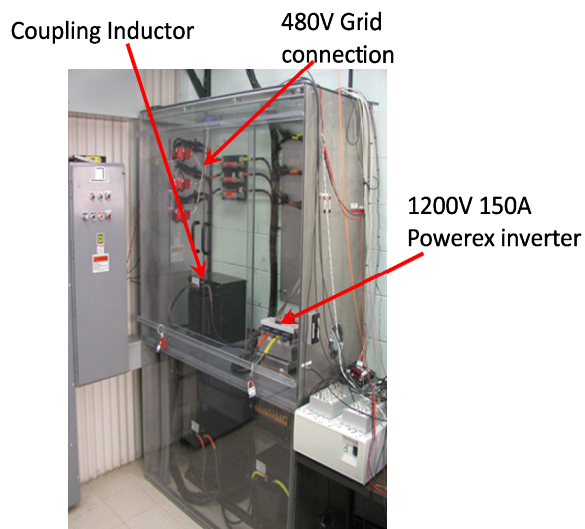


Figure 7. STATCOM setup at ORNL.

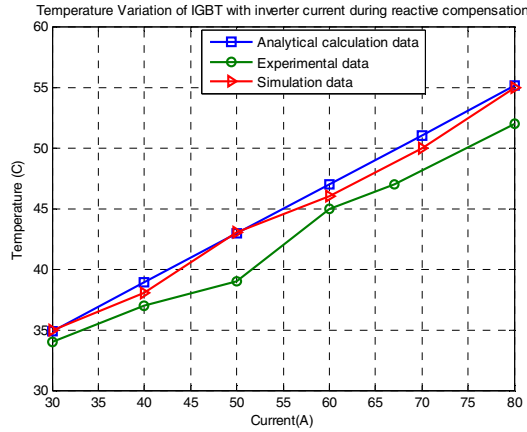


Figure 8. Comparison of temperature data at different inverter loads for reactive compensation by analytical calculation, simulation and experimental results.

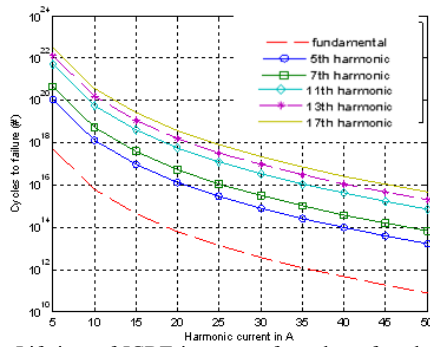


Figure 10. Lifetime of IGBT in terms of number of cycles to failure varying with harmonic current amplitude in semilog scale for the case when STATCOM provides harmonic compensation of a single harmonic.

Considering similar conditions, for the CM150DU IGBT phase leg module, rated at 1200V and 150A, the testing for the IGBT would be conducted at 1Hz [5, 6, 15]. A switching frequency of 1 kHz. for the PWM switching, would be a good choice to ensure near-operation condition. The test conditions are described in Table III.

### VII. PRELIMINARY RESULTS

Fig. 11 demonstrates the load current of power cycling circuit for a load current of 8A, switching frequency of 1 kHz, output frequency of 1Hz, input voltage of 13.8 V. FLIR infrared thermal camera was used to observe the temperature distribution. Fig. 12 demonstrates the temperature of IGBT with the above mentioned conditions. A slight variation in temperature was observed at low currents with heatsink.

Fig.13 shows the temperature distribution in the two modules of the full bridge inverter. The temperature is higher on the busbar connections where wirebonds are connected.

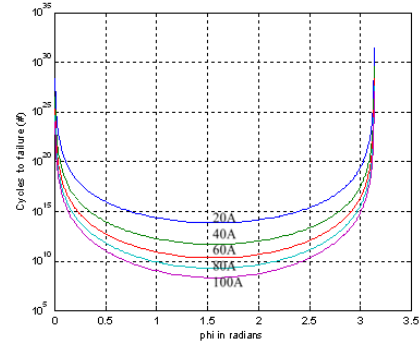


Figure 9. Lifetime of IGBT in terms of number of cycles to failure varying with power factor angle of the load.

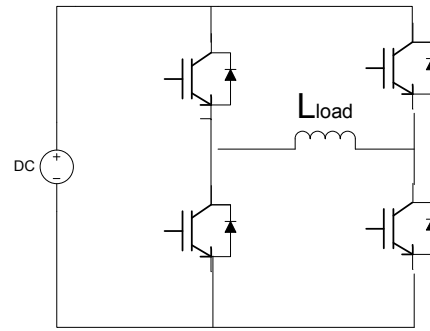


Figure 11. H-bridge inverter for power cycling.

TABLE III POWER CYCLING TEST CONDITIONS

Switching frequency, $f_s$	1kHz – 4 kHz
Output frequency, $f_o$	1-10 Hz
Input DC voltage, $V_{dc}$	<50 V
Load inductance, $L_{load}$	5-20 mH

Further analysis into the temperature distribution would give an insight to the failures.

### VIII. CONCLUSION

The impact of power factor correction and harmonic elimination on the temperature of IGBT is presented through analytical calculations, simulation and by experimental results. The lifetime of IGBT is calculated for a STATCOM operating for power factor correction and harmonic compensation.

1. As the power factor of the load decreases, the inverter losses increase, and the temperature increase is inverted parabolic in shape with a maximum temperature rise at  $\Phi = 90^\circ$ . The losses in the inverter are proportional to the load current and the power factor angle. The lifetime of the IGBT is inversely related to the temperature.

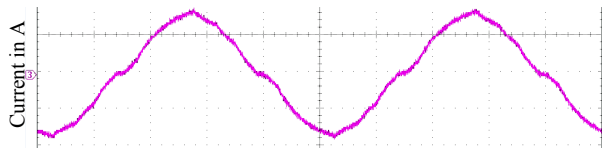


Figure 12. Load current of power cycling circuit for a load current of 8A, switching frequency of 1 kHz, output frequency of 1Hz, input voltage of 13.8 V. Current scale 5A/division

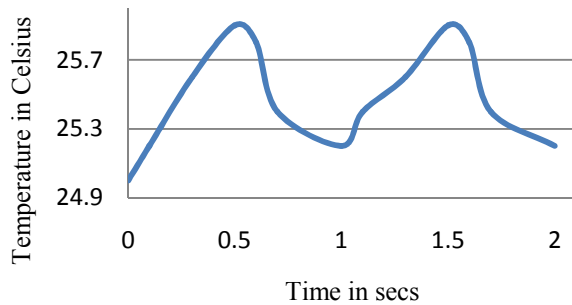


Figure 13. Junction temperature variation of IGBT for the 8A current of inductive load in H-bridge inverter.

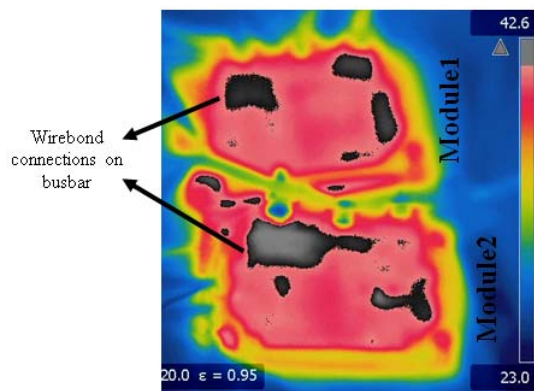


Figure 14. Thermal image of two modules in the full bridge inverter.

2. The losses due to harmonic compensation of purely harmonic load are independent of the frequency of the harmonics and dependent on the amplitude of the harmonic. The lifetime of the IGBT when compensating for higher order harmonic currents is higher than that of compensating the fundamental and lower harmonic currents.

For future consideration, the temperature profile for a grid load system and lifetime prediction using rainfall counting algorithm is proposed. Also, the lifetime of the diode compared with the IGBT for purely inductive loads is intended to be studied.

#### ACKNOWLEDGMENT

We would like to thank Powerex for their assistance with power cycling data of the module.

This work made use of Engineering Research Center Shared Facilities supported by the Engineering Research Center Program of the National Science Foundation and DOE under NSF Award Number EEC-1041877 and the CURENT Industry Partnership Program.

#### REFERENCES

- [1] North American Electric Reliability Corporation "Reliability Considerations from Integration of Smart Grid," Report, Dec.2010.
- [2] J. Liu and N. Henze, "Reliability consideration of low-power grid-tied inverter for photovoltaic application", *24th European Photovoltaic Solar Energy Conference and Exhibition*, Hamburg/Germany, 21.-25. September 2009.
- [3] M. Ciappa, W. Fichtner, F. Carbognani, "Lifetime Prediction and Design of Reliability Tests for High-Power Devices in Automotive Applications," *IEEE Transactions on Device and Materials Reliability*, Dec. 2003, vol. 3, pp. 191 – 196.
- [4] J. J. Rodríguez, Z. Parrilla, M. Veléz-Reyes, A. Hefner, D. Berning, J. Reichl, and J. Lai, "Thermal Component Models for Electro Thermal Analysis of Multichip Power Modules," *Proceedings of IEEE Industry Applications Society Meeting*, October 2002, pp. 234-241.
- [5] L. Wei, R. J Kerkman, R. A. Lukaszewski, "Evaluation of Power Semiconductor Power Cycling Capabilities for Adjustable Speed Drive," *Proc. IEEE IAS 2008 conference*, Edmonton, Canada, 2008.
- [6] L. Wei, T. Lipo, R. A. Lukaszewski, "Analysis of Power Cycling Capability of IGBT Modules in a Conventional Matrix Converter," *Proc. IEEE IAS conference*, Edmonton, Canada, 5-9 Oct. 2008, pp. 1 – 8.
- [7] A. Hefner, H Mantooh, "Electrothermal simulation of an IGBT PWM inverter," *IEEE Transactions on Power Electronics*, May 1997, vol. 12, pp. 474 – 484.
- [8] Yan Xu, "A Generalized Instantaneous Non-active Power Theory for Parallel Nonactive Power Compensation," A Dissertation Presented for the Doctor of Philosophy Degree, The University of Tennessee, Knoxville, May 2006.
- [9] B. Ozpineci, L. Tolbert, S. Islam, Md. Hasanuzzaman, "Effects of Silicon Carbide (SiC) Power Devices on HEV PWM Inverter Losses," *the 27th Annual Conference of the IEEE Industrial Electronics Society*, 2001, vol. 2, pp. 1061- 1066.
- [10] [www.emtp.com](http://www.emtp.com)
- [11] M. Held, P. Jacod, P.Scacco, and M. Poech, "Fast Power Cycling Test for IGBT Modules in Traction Application", *International Conference on Power Electronics and Drives Systems*, May ,1997, vol. 1, pp. 425-430.
- [12] A. Bueta, "A Novel Test Method For Minimising Energy Costs In IGBT Power Cycling Studies," Dissertation Doctor of Philosophy, the University of the Witwatersrand, Johannesburg, 2006.
- [13] L. GopiReddy, L. Tolbert, B. Ozpineci, Y. Xu, D.T. Rizy, "Impact of Power Factor Correction and Harmonic Compensation by STATCOM on Converter Temperature," *ECCE 2011*, Sept. 17-22, Phoenix, USA, pp. 1928 – 1934.
- [14] S. Yang, A. T. Bryant, P. A. Mawby, D. Xiang, L. Ran, and P. Tavner, "An industry-based survey of reliability in power electronic converters," *IEEE Transactions on Power Electronics*, Nov.2010, vol. 25, pp. 2734-2752.
- [15] M. Mussallam, C. M. Johnson , " Real-time Thermal Models for Health Management of Power Electronics," *IEEE Transactions on Power Electronic*, June 2010, vol. 25, pp. 1416-1425.